## WIND-SHEARING IN GASEOUS PROTOPLANETARY DISKS AND THE EVOLUTION OF BINARY PLANETESIMALS

HAGAI B. PERETS AND RUTH A. MURRAY-CLAY Harvard-Smithsonian Center for Astrophysics, 60 Garden st. Cambridge MA 02338, USA Draft version September 12, 2018

#### ABSTRACT

One of the first stages of planet formation is the growth of small planetesimals and their accumulation into large planetesimals and planetary embryos. This early stage occurs much before the dispersal of most of the gas from the protoplanetary disk. Due to their different aerodynamic properties, planetesimals of different sizes and shapes experience different drag forces from the gas during this time. Such differential forces produce a wind-shearing (WISH) effect between close by, different size planetesimals. For any two planetesimals, a WISH radius can be considered, at which the differential acceleration due to the wind becomes greater than the mutual gravitational pull between the planetesimals. We find that the WISH radius could be much smaller than the gravitational shearing radius by the star (the Hill radius). In other words, during the gas-phase of the disk, WISH could play a more important role than tidal perturbations by the star. Here we study the WISH radii for planetesimal pairs of different sizes and compare the effects of wind and gravitational shearing (drag force vs. gravitational tidal force). We then discuss the role of WISH for the stability and survival of binary planetesimals. Binaries are sheared apart by the wind if they are wider than their WISH radius. WISH-stable binaries can also inspiral, and possibly coalesce, due to gas drag. Here, we calculate the WISH radius and the gas drag-induced merger timescale, providing stability and survival criteria for gas-embedded binary planetesimals. Our results suggest that even WISH-stable binaries may merge in times shorter than the lifetime of the gaseous disk. This may constrain currently observed binary planetesimals to have formed far from the star or at a late stage after the dispersal of most of the disk gas. We note that the WISH radius may also be important for other processes such as planetesimal erosion and planetesimal encounters and collisions in a gaseous environment.

#### 1. INTRODUCTION

Gravitational encounters between planetesimals play an important role in the evolution of protoplanetary disks and planet formation (e.g., reviews by Lissauer 1993; Goldreich et al. 2004). Planetesimal growth likely occurs while the planetesimals are still embedded in a gaseous disk. Studies of gas-planetesimal interactions have shown that gas can affect the velocity dispersion of planetesimals (e.g. Nelson & Gressel 2010), may help the formation of large planetesimals through clumping of planetesimals (Chiang & Youdin 2010, and references therein), and can lead to fast inspiral of planetesimals into the star through gas-drag (Nakagawa et al. 1986; Weidenschilling 1977, and references therein). Here we focus on a different aspect of planetesimals embedded in a gaseous disk, namely the close interaction between pairs of single planetesimals in a gaseous environment.

Planetesimals likely vary in size and shape, and therefore have a wide range of aerodynamical properties, which affect their interaction with surrounding gas. In particular, planetesimals of different sizes and/or shapes experience different drag forces from the head wind they encounter in the gaseous disk. The difference between the forces acting on two different-size planetesimals (Weidenschilling 1977) can change their relative trajectories with respect to their unperturbed motion in the absence of gas (for example Ormel & Klahr 2010 considered planetesimal interactions in gas rich environment; their study focused on planar encounters and drag law regimes which are linearly dependent on velocity).

During an encounter between two different-size plan-

etesimals, the different forces experienced by the two components as a result of gas drag generate a wind-shearing (WISH) effect, which could be stronger than their gravitational interaction. For any two planetesimals, we consider the radius, which we term the WISH radius, at which the differential acceleration due to aero-dynamical wind-shearing becomes greater than the mutual gravitational pull between them. In the following we explore this new distance scale and discuss its implications, including the stability of binary planetesimals. In addition, we study the evolution of WISH-stable binary planetesimals in gas. Such binaries dissipate their orbital energy through gas drag and may inspiral to form closer binaries or even coalesce during the typical lifetime of a protoplanetary disk.

We begin by deriving the WISH radius and discussing the effects of gas drag on particles of different sizes. We then calculate the WISH radius for two planetesimals of arbitrary effective sizes (Section 2). In Section 3, we consider the evolution of binary planetesimals embedded in a gas disk, including WISH stability (Section 3.1) and gas drag-induced inspiral (Section 3.2). Finally, we discuss various other possible implications of our results (Section 4) and summarize (Section 5).

# 2. GAS DRAG AND THE WIND-SHEARING RADIUS IN PROTOPLANETARY DISKS

Planetesimals of different sizes embedded in the same gaseous environment experience different drag forces and hence different accelerations. The differential acceleration between two planetesimals of mass  $m_b$  and  $m_s$  due to the wind-shearing effect is given by

$$\Delta a_{WS} = \left| \frac{F_D(m_b)}{m_b} - \frac{F_D(m_s)}{m_s} \right| = \frac{3\rho_p}{4\pi} \left| \frac{F_D(r_b)}{r_b^3} - \frac{F_D(r_s)}{r_s^3} \right|,\,$$
(1)

where  $F_D$  is the force exerted on a particle due to gas drag. Throughout this paper, we perform our calculations for spherical particles of constant density,  $\rho_p$ , so that the mass of a planetesimal with radius r is  $m = (4/3)\pi\rho_p r^3$ . In Equation (1), planetesimal masses  $m_b$  and  $m_s$  correspond to radii  $r_b$  and  $r_s$ , respectively. Real planetesimals could have different aerodynamical properties (e.g. they may not be spherical and/or they could be porous); however, calculations analogous to those presented here may be performed for any form of  $F_D(m)$ .

For small separations over which the environmental conditions (gas density and temperature) are approximately the same, the differential WISH acceleration between any two planetesimals is independent of the distance between them. In this case,  $\Delta a_{WS}$  can be used to define an important distance scale, which we term the WISH radius. To define this scale, we adopt a similar approach to that used to define the the gravitational tidal-shearing radius, i.e., the Hill radius.

The Hill radius (sphere) is the distance at which the gravitational influence of a planetesimal or a planet with mass m and radius r, orbiting a star with mass  $M_{\star}$  at radial distance a, becomes comparable to the tidal perturbation by the star. It is given by

$$R_H = \left(\frac{m}{3(M_{\star} + m)}\right)^{1/3} a \simeq \left(\frac{4\pi\rho_p}{9M_{\star}}\right)^{1/3} ra,$$
 (2)

where the second expression is derived for a spherical planetesimal with  $m \ll M_{\star}$ . A test particle located close to the Hill radius, or beyond it, is strongly affected by the gravitational pull of the star. If it begins in orbit around the planetesimal, its orbit will be perturbed and is likely to become unstable. The exact distance up to which a binary orbit can remain stable also depends on its orbit direction, e.g. prograde or retrograde with respect to the orbit of the planet around the star (Hamilton & Burns 1991; Shen & Tremaine 2008; Perets & Naoz 2009), or more generally, the relative inclination of the particle's orbit. In the following we adopt the simple definition given by Eq. (2).

Following the definition of the Hill radius we can now define the WISH radius. This radius is defined as the distance between two planetesimals for which the differential WISH acceleration between them equals their mutual gravitational pull. Equating  $\Delta a_{WS}$  with the gravitational acceleration  $a_{grav} = G(m_b + m_s)/d_{bin}^2$  yields a separation  $d_{bin}$  between the two planetesimals equal to the WISH radius, which we define as

$$R_{WS} = \sqrt{\frac{G(m_b + m_s)}{\Delta a_{WS}}}. (3)$$

Beyond this limiting radius even two planetesimals which are formally gravitationally bound (in the absence of WISH) would be sheared apart by the wind.

In order to calculate the specific value of the WISH radius for any given pair of planetesimals, we first need to understand the gas-drag force applied on planetesimals which face a head wind. This depends on the specific regime of the gas-planetesimal interaction, since different gas-drag laws apply under different conditions. We review gas drag laws in Section 2.1, calculate  $\Delta a_{WS}$  explicitly for several regimes in Section 2.2, and combine these to provide self-consistent calculations of  $R_{WS}$  as a function of planetesimal size in a fiducial disk (Section 2.3).

#### 2.1. Drag laws

The appropriate gas-drag force on a planetesimal of radius r moving through gas at relative velocity  $v_{rel}$  depends on  $r/\lambda$ , where  $\lambda = \mu/(\rho_g\sigma)$  is the mean free path of the gas,  $\sigma$  is the cross-section for gas-gas collisions, and  $\mu$  is the mean molecular weight. For planetesimals with diameters larger than the mean free path of the gas, the drag force also depends on the fluid Reynolds number  $Re = 2rv_{rel}/(0.5\bar{v}_{th}\lambda)$ . Here, 2r is the diameter of the planetesimal. The gas has kinematic viscosity  $(1/2)\bar{v}_{th}\lambda$ , temperature T, and mean thermal velocity (for a Maxwellian distribution)  $\bar{v}_{th} = (8/\pi)^{1/2}c_s$ , where  $c_s = (kT/\mu)^{1/2}$  is the sound speed and k is Boltzmann's constant. The various gas drag regimes can be summarized as follows (where we follow Weidenschilling 1977, who in turn follows Whipple 1973).

When  $r \lesssim \lambda$ , drag may be modeled by considering individual and independent particle collisions, and the Epstein regime applies (for subsonic  $v_{rel}$ , which is appropriate for our problem):

$$F_D = \frac{4}{3}\pi \rho_g \bar{v}_{th} v_{rel} r^2, \tag{4}$$

For  $r \gtrsim \lambda$ , the gas must be modeled as a fluid. We take  $r = (9/4)\lambda$  as the boundary between these regimes. At low Reynolds number, the gas/particle boundary layer dominates (Stokes drag), while at high Re, the gas exerts a Ram pressure force on the particle, so that the drag law is

$$F_D = 3\pi \rho_g \bar{v}_{th} v_{rel} \lambda r$$
 for  $Re < 1$  Stokes  
 $F_D = 0.22\pi \rho_g v_{rel}^2 r^2$  for  $Re \gtrsim 800$  Ram. (5)

An intermediate regime exists for  $1 \lesssim Re \lesssim 800$ . More generally, the full range of Reynolds numbers can be fitted with a drag law of

$$F_D = \frac{1}{2} C_D(R_e) \pi r^2 \rho_g v_{rel}^2$$
 (6)

where  $C_D(Re)$  can be fitted with an empirical formula based on recent experimental data in the regime  $10^{-3} \le Re \le 10^5$  (Brown & Lawler 2003; Cheng 2009; compati-

 $<sup>^1</sup>$  Planetesimals move through the protoplanetary disk at subsonic velocities. For  $v_{rel}>c_s,\ {\rm ram}$  pressure drag applies (c.f. Equation 5).

ble with older data used by Whipple 1973), yielding

$$C_D = \frac{24}{Re} (1 + 0.27Re)^{0.43} + 0.47[1 - exp(-0.04Re^{0.38})].$$
(7)

We use Equations (6) and (7) for our drag law in the calculations that follow, except when a single, specific drag law is specified, in which case we use Equations (4) and (5).

## 2.2. The wind-shearing differential acceleration

When two particles with radii  $r_b$  and  $r_s$  experience gas drag in the same drag regime, we may obtain a simple expression for the wind-shearing differential acceleration,  $\Delta a_{WS}$ . For example, in the Epstein regime  $(r_s, r_b < \lambda)$ ,

$$\Delta a_{WS} = \frac{4}{3} \pi \rho_g \bar{v}_{th} \left| \frac{r_b^2 v_{rel}(r_b)}{m_b} - \frac{r_s^2 v_{rel}(r_s)}{m_s} \right| \qquad Epstein.$$
(8)

In general, the relative velocity between each of the planetesimals and the gas could differ, in which case even planetesimals of the same size can experience a differential WISH acceleration. For bound binary planetesimals (which we discuss in Section 3.1) the velocity relative to the gas of the two components should be, on average, approximately the same, so that  $v_{rel} = v_{rel}(r_b) = v_{rel}(r_s)$ . In this case, Eq. (8) simplifies further:

$$\Delta a_{WS} = \rho_g \bar{v}_{th} v_{rel} \left| \frac{r_b^2}{r_b^3 \rho_p} - \frac{r_s^2}{r_s^3 \rho_p} \right|$$

$$= \frac{\rho_g}{\rho_p} \frac{\bar{v}_{th} v_{rel}}{r_s} \left| \frac{r_s}{r_b} - 1 \right|$$

$$\simeq \frac{\rho_g}{\rho_p} \frac{\bar{v}_{th} v_{rel}}{r_s} , \quad Epstein$$
 (9)

where the last expression is for  $r_b \gg r_s$ . Similarly, under the same assumptions, the Stokes regime produces

$$\Delta a_{WS} \simeq 3\pi \rho_g \bar{v}_{th} v_{rel} \lambda \left(\frac{r_s}{m_s}\right)$$

$$= \frac{9}{4} \frac{\mu}{\rho_p \sigma} \frac{\bar{v}_{th} v_{rel}}{r_s^2}, \quad Stokes \tag{10}$$

and in the Ram pressure regime,

$$\Delta a_{WS} \simeq 0.22\pi \rho_g v_{rel}^2 \left(\frac{r_s^2}{m_s}\right)$$

$$= 0.165 \frac{\rho_g}{\rho_p} \frac{v_{rel}^2}{r_s}. \quad Ram$$
(11)

We note that in the Stokes regime,  $\Delta a_{WS}$  does not depend on the density of the gas.

More generally, the differential acceleration can be obtained accurately for any combination of two planetesimals in different drag law regimes and moving through the gas at different velocities. This can be done by using Eqs. (4) and (5) or Eqs. (6) and (7) to calculate the appropriate drag force on each planetesimal.

## 2.3. The wind-shearing radius

Given the expressions in Equations (9)–(11), we can obtain relatively simple formulas for the wind-shearing

radius (Equation 3) for two planetesimals in the same drag law regime with  $v_{rel}(r_b) = v_{rel}(r_s)$  and  $r_b \gg r_s$ :

$$R_{WS} = \sqrt{\frac{G(m_b + m_s)}{\Delta a_{WS}}} \approx \sqrt{\frac{Gm_b}{\Delta a_{WS}}}$$

$$= (Gm_b \rho_p)^{1/2} \times \begin{cases} \left(\frac{1}{\rho_g \bar{v}_{th} v_{rel}}\right)^{1/2} r_s^{1/2} & Epstein, \\ \left(\frac{4}{9} \frac{\sigma}{\mu \bar{v}_{th} v_{rel}}\right)^{1/2} r_s & Stokes, \\ \left(\frac{1}{0.165} \frac{1}{\rho_g v_{rel}^2}\right)^{1/2} r_s^{1/2} & Ram, \end{cases}$$

in the Epstein, Stokes, and Ram pressure regimes, respectively. In fact, these expressions apply as long as the gas accelerates the smaller body more effectively than the larger body, even if their drag regimes are different. In this case the drag regime in Eq. (12) would correspond to that of the smaller body.

More generally, we can calculate  $R_{WS}$  for any two planetesimals of arbitrary size (in the same or in different gasdrag regimes) as a function of the properties of the gas in which they are embedded. When  $r_b < R_{WS} < R_H$ , the WISH radius represents the limiting separation of a binary planetesimal (or a pair of small satellites) in a gaseous environment.

In Figure 1, we show the calculated  $R_{WS}$  and the resulting binary stability radius for a planetesimal with radius  $r_b = 10$  km, orbited by a smaller body with a range of sizes. This calculation is performed at 1 AU from a solar-mass star in a disk having the following parameters. We choose a disk temperature of  $T=T_0(a/{\rm AU})^{-3/7}$  with  $T_0=120\,$  K, following Chiang & Youdin (2010), who adapt the results of Chiang & Goldreich (1997) for a disk around the young Sun. Varying the value of  $T_0$  within a reasonable range for Sun-like stars does not qualitatively change our results. We take the surface density of the disk to be  $\Sigma_g = \Sigma_0 (a/\mathrm{AU})^{-1}$ , with  $\Sigma_0 = 2 \times 10^3 \ \mathrm{g/cm^2}$ . This choice is roughly consistent with the minimum-mass solar nebula at 1 AU as well as with observed dust surface density profiles at distances larger than  $\sim 20~\mathrm{AU}$ in extrasolar disks, taking a dust to gas mass ratio of 1:100 (typically assumed in the modeling of protoplanetary disks, e.g. Andrews et al. 2010). Protoplanetary disks likely exhibit a range of surface density profiles across different systems and at different times within the same system. We discuss the impact of varying the gas surface density in the Appendix.

Given the above choices, the disk scale height H is given by

$$\frac{H}{a} \sim \frac{c_s}{\Omega a} \sim 0.022 \left(\frac{a}{AU}\right)^{2/7},\tag{13}$$

where  $\Omega = (GM_{\star}/a^3)^{1/2}$  is the Keplerian orbital frequency. The gas volume density profile is then

$$\rho_g \sim \frac{\Sigma_g}{2H} \sim 3 \times 10^{-9} \left(\frac{a}{AU}\right)^{-16/7} \text{ g/cm}^3.$$
(14)

Using the neutral collision cross-section  $\sigma \sim (3\text{Å})^2 \sim$ 

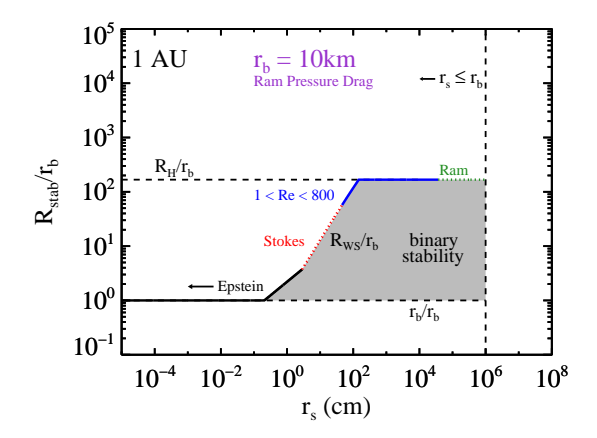


Figure 1. The binary stability radius for a  $r_b=10$  km planetesimal with a companion of radius  $r_s < r_b$ , at 1 AU from the star in our fiducial disk. At radii between the physical size and the Hill radius of the large planetesimal (lower and upper dashed lines, respectively), the stability radius equals the WISH radius,  $R_{WS}$  (see text). The planetesimals are moving at a relative velocity of  $v_{rel} \approx 0.5 c_s^2/v_K$  with respect to the gas. The relevant drag regime for the small body changes with  $r_s$ , and the WISH radius is well approximated by Equation (12). A pair of bound planetesimals (a binary) can only exist in the shaded region; it can not reside lower than the physical size (collision), above the Hill radius (gravitationally unbound by tidal shearing from the star) or to the left of the WISH radius (sheared apart by the wind).

 $10^{-15}$  cm<sup>2</sup>, the mean free path of the gas is

$$\lambda \sim \frac{1}{n_g \sigma} \sim 1 \left(\frac{a}{AU}\right)^{16/7} \text{ cm}$$
 (15)

where the gas number density  $n_g = \rho_g/\mu$  and we have used  $\mu = 2.3m_H$  with  $m_H$  equal to the mass of a hydrogen atom.

For these calculations, we assume that the relative velocity between the binary and the gas is equal to the velocity of a single planetesimal with radius equal to that of the larger component of the binary,  $r_b$ , as it moves through a smooth disk under the influence of gas drag. This approximation is valid for  $r_b \gg r_s$ . In reality, a bound binary will move through the gas at a velocity that reflects the drag on both binary components. Following Youdin (2010; see also Nakagawa et al. 1986), we set the relative velocity between a planetesimal and the gas to be  $v_{rel} = (v_{rel,r}^2 + v_{rel,\phi}^2)^{1/2}$  with

$$v_{rel,r} = -2\eta v_K \left[ \frac{t_s \Omega}{1 + (t_s \Omega)^2} \right] \tag{16}$$

$$v_{rel,\phi} = -\eta v_K \left[ \frac{1}{1 + (t_s \Omega)^2} - 1 \right]$$
 (17)

with  $\eta \equiv (v_K - v_{g,\phi})/v_K$ , so that  $\eta v_K$  equals the difference between the azimuthal gas velocity,  $v_{g,\phi}$ , and the Keplerian velocity,  $v_K = \Omega a$ . We use the approximate value  $\eta = 0.5(c_s^2/v_K^2)$ . We calculate the stopping time  $t_s = m v_{rel}/F_D$  and relative velocity  $v_{rel}$  of a planetesimal iteratively, using the drag law in Equation (7), in order to achieve self-consistent values for these and hence for  $F_D$  in all drag regimes. Note, however, that our choice of  $v_{rel}$  represents the velocity of a planetesimal moving through a uniform disk and does not take into account turbulence. In addition, even in a smooth disk planetes-

imal growth likely occurs in regions of enhanced solids, which may accelerate the disk gas to more nearly Keplerian speeds, reducing this relative velocity. We discuss how our results vary as a function of relative velocity in the Appendix.

Under our assumed conditions, a 10 km planetesimal at 1 AU orbits at approximately the Keplerian velocity, so that in Figure 1,  $v_{rel} \approx 0.5 c_s^2/v_K$ . At this relative velocity, the Reynolds number for a planetesimal with radius  $r_s$  is

$$Re = \frac{2r_s v_{rel}}{0.5 \bar{v}_{th} \lambda} \sim \sqrt{\frac{\pi}{2}} \frac{r_s}{\lambda} \frac{c_s}{v_K} \sim \left(\frac{\lambda}{r_s}\right)^{-1} \left(\frac{H}{a}\right)$$
$$\sim 0.02 \left(\frac{r_s}{1 \text{ cm}}\right) \left(\frac{a}{AU}\right)^{-2} \tag{18}$$

The transition from the Epstein to the Stokes regime for the small planetesimals may be clearly seen in Figure 1 as a change in the slope of the WISH radius from 1/2 to unity. This behavior is matched by Eq. (12). Though the large body in this plot always remains in the Ram pressure drag regime, it is not accelerated much by the gas, and  $\Delta a_{WS}$  is dominated by the acceleration of the small companion. The agreement between these results and Eq. (12) reflects the fact that in this regime, the small companions are accelerated more effectively by the gas than the 10 km large body.

Figure 2 displays the calculated WISH radius as a function of the small planetesimal size for various sizes of the large planetesimal and at different distances from the star. Also shown for comparison are the physical size of the big planetesimal and its Hill radius. The WISH radius diverges for equal size planetesimals (with the same velocities relative to the gas), since they experience the same gas drag, and their differential WISH acceleration approaches zero.

## 3. BINARY PLANETESIMALS IN A GASEOUS ENVIRONMENT

A non-negligible fraction of currently observed planetesimals in the Solar system (including asteroids and Trans-Neptunian objects) are found to be members of binaries (e.g., Richardson & Walsh 2006; Noll et al. 2008). Binary planetesimals can teach us about the dynamical evolution of the Solar system (Perets & Naoz 2009; Murray-Clay & Schlichting 2011; Parker & Kavelaars 2010) and can play a role in planet formation and planetesimal growth (Nesvorný et al. 2010; Perets 2010). Study of the interactions of binary planetesimals with gas is therefore important for understanding the formation, stability and evolution of these binaries and their implications. In the following we discuss the effect of WISH and gas drag inspiral and coalescence of binary planetesimals in gas.

#### 3.1. Wind-shearing disruption of binary planetesimals

We have already alluded to an immediate consequence of the wind-shearing radius for binary planetesimals, namely that it provides a new stability criterion for their survival (see Figure 1). In a gas free environment, binary planetesimals are stable as long as their separation is smaller than the Hill radius, whereas wider binaries are destabilized and disrupted by the tidal gravitational shearing from the star. However, in the presence of gas,

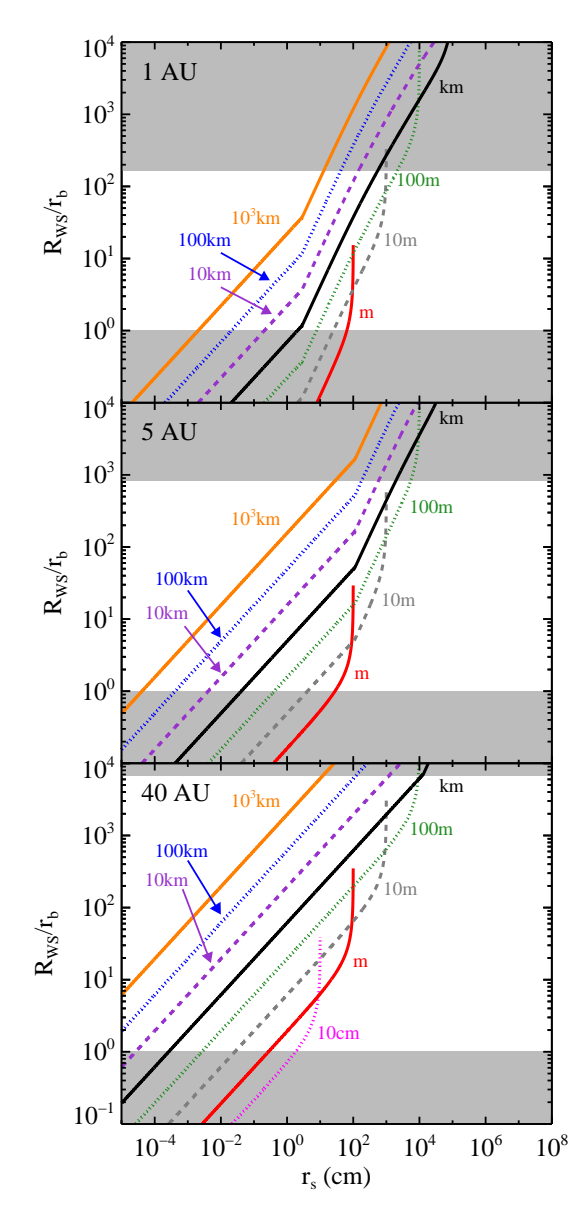


Figure 2. The WISH radius,  $R_{WS}$ , (see text and Figure 1) for two planetesimals of sizes  $r_s$  and  $r_b$  as a function of  $r_s$ , at distances of 1, 5 and 40 AU from the star (top, middle, and lower panels, respectively). The plotted lines show  $R_{WS}$  for planetesimals with radii  $r_b = 10^{-1} - 10^8$  cm, in logarithmic jumps. The shaded regimes show the regions where the WISH radius is smaller than the physical radius or larger than the Hill radius of the big planetesimal. We do not show lines corresponding to big planetesimals for which the WISH radius is smaller than the physical radius unless the smaller planetesimal nearly equals the larger planetesimal in size (e.g.  $r_b < 1$  m at 1 and 5 AU).

the Hill radius stability limit should be replaced by the WISH radius when  $R_{WS} < R_H$  (binaries wider than the Hill radius are always unstable). We find that the stability criterion for binaries embedded in gas is

$$d_{bin} \le \min(R_H, R_{WS}). \tag{19}$$

Because collisions prevent binaries from forming with  $d_{bin} < r_b$ , no stable binaries are possible when  $R_{WS} < r_b$ . Given these considerations, the limiting separations of binary planetesimals in our fiducial disk as a function of size and distance from the star may be read from Fig-

ure 2 (see also Figure 1). For planetesimal sizes spanning a wide range,  $r_b < R_{WS} < R_H$  in our fiducial disk and this limiting separation is equal to the WISH radius. Binary planetesimals can therefore be strongly affected by WISH, most notably for smaller planetesimals closest to the star. Generally we find that for a wide range of binary and disk properties the WISH radius determines the stability rather than the Hill radius. A gaseous environment qualitatively changes the spatial dependence of binary stability in a protoplanetary disk, as the spatial dependence (distance from the star) of the Hill radius and that of the WISH radius differ. This can be seen in Figure 3, which compares the WISH radius with the Hill radius for a given binary pair as a function of the distance from the star (also compare the panels in Figure 2). We note that binaries with radii of  $\sim 100 \text{ km}$ and components of roughly equal mass, comparable to many observed Trans-Neptunian and asteroid binaries, have their stability determined by the Hill radius at all distances from the star in our fiducial disk.

More details regarding the dependence of our results on the gas density and the relative velocity of planetesimals with respect to the gas can be found in the Appendix.

## 3.2. Gas drag-induced inspiral of binary planetesimals

Many studies have demonstrated that single planetesimals inspiral toward their host star due to gas drag (e.g., Weidenschilling 1977; for a review see Chiang & Youdin 2010 and references therein). A similar process can cause the inspiral of a binary planetesimal into a closer mutual orbit, possibly ultimately leading to coalescence. In the following we explore the evolution of the mutual orbits of binary planetesimals in gas, and we provide the timescales for their coalescence.

For simplicity we restrict our discussion to binary planetesimals with  $m_s \ll m_b$ , but our results can be simply generalized to arbitrary mass ratios. We study the evolution of a binary orbiting the Sun in the plane of the protoplanetary disk. For simplicity, we assume throughout that the mutual binary orbit begins circular and dissipates orbital energy on a timescale much longer than the mutual orbital period. The two components of the binary therefore orbit one another on roughly circular trajectories at a (shrinking) binary separation of  $d_{bin}$ . In some circumstances binaries can evolve on faster timescales; such short term evolution relates to binary planetesimal formation through gas dissipation and may result in fast coagulation of planetesimals. These latter processes will be discussed elsewhere (see Murray-Clay & Perets, in preparation).

In this limit, the binary loses angular momentum L on a timescale of  $|L/\dot{L}| = m_s v_{bin}/\langle F_D \rangle$ , where  $v_{bin}$  is the binary orbital velocity of the small body and  $\langle F_D \rangle$  is the gas drag force on the small body, averaged over a binary orbital period. Equivalently, the binary loses orbital energy E on a timescale of  $|E/\dot{E}| = 0.5 m_s v_{bin}^2/(\langle F_D \rangle v_{bin})$ . Inspiral therefore proceeds on a timescale  $\tau_{\rm merge} \equiv d_{bin}/\dot{d}_{bin} = (1/2)L/\dot{L} = E/\dot{E}$ , so that

$$\tau_{\text{merge}} = \frac{d_{bin}}{\dot{d}_{bin}} = \frac{1}{2} \frac{m_s v_{bin}}{\langle F_D \rangle} \tag{20}$$

In calculating the gas drag force, we must average over an orbital period because the center of mass of the binary

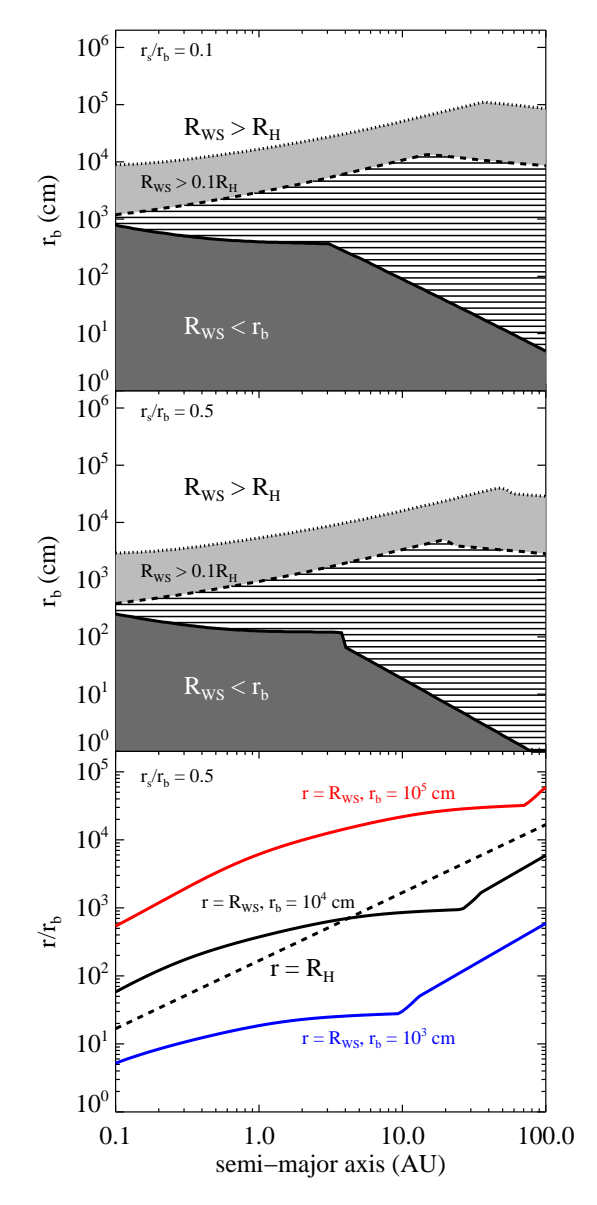


Figure 3. Comparison of the WISH radius and the Hill radius as a function of planetesimal size and distance from the star. The WISH radius restricts binary stability most at larger separations, where the tidal force from the star becomes weak. The planetesimal size for which  $R_{WS}(r_b) = R_H(r_b)$  (dotted line),  $R_{WS} = 0.1R_H$  (dashed line) and  $R_{WS}(r_b) = r_b$  (solid line), as a function of the distance from the star, for a binary planetesimal with size ratio  $r_s/r_b = 0.1$ . Middle panel: Same a top panel, but for  $r_s/r_b = 0.5$ . Larger size ratios reduce the impact of WISH, making binaries more stable. Binaries in the bottom shaded region can not survive WISH and will be disrupted by the wind. The stability of binaries in the top region (above the  $R_W=R_H$  line) is set by the Hill radius rather than by the WISH radius, i.e. in that region gravitational shearing is stronger than WISH. Bottom panel: The binary WISH stability radius as a function of the distance from the star for three binaries with a size ratio  $r_s/r_b=0.5$ , and primaries of  $r_b=1\,$  km (top red solid line),  $r_b=0.1\,$  km (middle black solid line) and  $r_b = 0.01$  km (bottom blue solid line). Also shown (dashed line) is the spatial linear dependence of the Hill radius, corresponding to the stability radius for a non-gaseous planetesimal disk. Note that  $R_H/r_b$  is independent of  $r_b$ .

is moving with respect to the background gas with relative velocity  $v_{disk}$  as it orbits the Sun. Given  $m_s \ll m_b$ , the relative velocity between the binary and the disk gas is approximately the velocity at which the large body would move through the gas on its own, given by Equations (16) and (17).

We now provide analytic expressions for the infall time in two different gas-drag regimes, the regime which is linear in velocity (corresponding to the Stokes and Epstein regimes; Section 3.2.1) and the quadratic (ram pressure) regime (Section 3.2.2). In the quadratic regime, the type of evolution depends on the ratio  $v_{bin}/v_{disk}$ . In practice more complicated regimes exist (see Section 2.1), which we integrate numerically for parameters relevant to planetesimals in a protoplanetary disk in Section 3.2.3.

#### 3.2.1. Linear drag regime

In the following treatment, we assume that  $v_{bin}$  remains constant over a single binary orbital period  $P_{\text{bin}}$ , which is good for  $v_{bin}/\dot{v}_{bin} \gg P_{\text{bin}}$ . Note that this assumption requires not only that  $\tau_{\text{merge}} \gg P_{\text{bin}}/2$  but also that  $m_s v_{bin}/F_{D,disk} \gg P_{\text{bin}}$ , where  $F_{D,disk}$  is the drag force experienced by the small body moving at relative velocity  $v_{disk}$  with respect to the gas. We address the complication of non-circular orbits in future work.

In the linear regime,  $F_D \propto v_{rel}$ , with  $v_{rel}$  equal to the relative velocity of the small body with respect to the gas, containing components from the binary orbit and from the overall motion of the binary through the gas disk. Therefore  $F_{D,1} \equiv F_D/v_{rel}$  is constant over the binary orbit. The linear regime is valid for the Epstein and Stokes drag regimes, but the value of  $F_{D,1}$  in the two regimes differs (see Section 2.1). We may now express the orbit-averaged drag force as

$$\langle F_D \rangle = \frac{1}{2\pi} \int_0^{2\pi} F_D d\theta$$

$$= \frac{F_{D,1}}{2\pi} \int_0^{2\pi} (v_{bin} \sin \theta + v_{disk}) d\theta = F_{D,1} v_{bin} ,$$
(21)

where  $\theta$  is the angle of the binary in its orbit. The term  $v_{bin} \sin \theta$  is the bulk velocity component of the small planetesimal parallel to the direction of motion in the binary frame of reference, so that  $v_{rel} = v_{bin} \sin \theta + v_{disk}$ . Over a full orbit the contribution from  $v_{disk}$  averages out and

$$\tau_{\text{merge}} = \frac{t_{stop}}{2} ,$$
(22)

with  $t_{stop}$  equal to the stopping time of a single small planetesimal in the gaseous protoplanetary disk:

$$t_{stop} = \frac{m_s}{F_{D,1}} = \begin{cases} \left(\frac{\rho_p}{\rho_g}\right) \frac{r_s}{\bar{v}_{th}} & Epstein \\ \frac{4}{9} \left(\frac{\rho_p}{\rho_g}\right) \frac{r_s^2}{\lambda \bar{v}_{th}} & Stokes. \end{cases}$$

Recall that in the linear regime, the stopping time is independent of the relative velocity between the planetesimal and the gas. Note that single planetesimals with stopping times longer than an orbital time inspiral into the star on a timescale of  $\sim t_{stop}/\eta$ . The same processes are at work in both cases—infall into the star is slower than

binary coalescence because the gas and planetesimals orbit the star together, reducing their relative velocities.

The timescale for coalescence is independent of  $d_{bin}$ , and the total merger time for a binary is

$$T_{merge} = \tau_{merge} \ln \left( \frac{d_0}{r_b} \right) ,$$
 (23)

where  $d_{bin} = d_0$  initially, and  $r_b$  is the final binary separation before coalescence.

#### 3.2.2. Quadratic (ram pressure) regime

We now consider the quadratic regime, for which  $F_D \propto v_{rel}^2$ , appropriate for ram pressure drag. Following the same procedure as above, but using  $F_{D,2} \equiv F_D/v_{rel}^2$  with  $F_{D,2}$  a constant, we get

$$\langle F_D \rangle = \frac{F_{D,2}}{2\pi} \int_0^{2\pi} (v_{bin} \sin \theta + v_{disk})^2 d\theta$$
$$= F_{D,2} v_{bin}^2 \left[ 1 + \frac{1}{2} \left( \frac{v_{disk}}{v_{bin}} \right)^2 \right]$$
(24)

In other words, the ram pressure drag force requires an effective relative velocity correction of  $[1 + 0.5(v_{disk}/v_{bin})^2]$ —in this case the contribution from the bulk velocity drag did not average out.

Now.

$$\tau_{\text{merge}} = \frac{t_{stop}(v_{bin})/2}{1 + 0.5(v_{disk}/v_{bin})^2},$$
(25)

where  $t_{stop}(v_{bin})$  is the stopping time for  $v_{rel} = v_{bin}$ . In the quadratic regime,  $t_{stop}$  is not independent of  $v_{rel}$ , so to make dependences clearer, we rewrite this expression as

$$\tau_{\text{merge}} = \frac{m_s / (2F_{D,2})}{v_{bin} [1 + 0.5(v_{disk} / v_{bin})^2]}$$

$$\approx \begin{cases} \frac{m_s}{2F_{D,2} v_{bin}} &, v_{bin} \gg v_{disk} \\ \frac{m_s v_{bin}}{F_{D,2} v_{disk}^2} &, v_{bin} \ll v_{disk} \end{cases}$$
(26)

Plugging in  $F_{D,2}$  for ram pressure drag and  $v_{bin} = (Gm_b/d_{bin})^{1/2}$ , this corresponds to

$$\tau_{\text{merge}} \approx \frac{2}{0.66} \left(\frac{\rho_p}{\rho_g}\right) r_s \times \left\{ \begin{array}{l} d_{bin}^{1/2} / \sqrt{Gm_b} &, v_{bin} \gg v_{disk} \\ 2\sqrt{Gm_b} / (d_{bin}^{1/2} v_{disk}^2), v_{bin} \ll v_{disk} \end{array} \right. \tag{27}$$

Integrating, we find a total merger time of

$$T_{merge} \approx \frac{2}{0.33} \left(\frac{\rho_p}{\rho_g}\right) r_s \times \begin{cases} \left(\frac{d_0^{1/2} - r_b^{1/2}}{\sqrt{Gm_b}}\right) &, v_{bin} \gg v_{disk} \\ \frac{2\sqrt{Gm_b}}{v_{disk}^2} \left(\frac{1}{r_b^{1/2}} - \frac{1}{d_0^{1/2}}\right), v_{bin} \ll v_{disk} \end{cases}$$
(28)

The merger time in the ram pressure regime depends strongly on the ratio between the binary mutual orbital velocity and its bulk velocity around the star. When  $v_{bin} \gg v_{disk}$ , the merger proceeds most slowly when  $d_{bin}$  is largest, while for  $v_{bin} \ll v_{disk}$ , the final coalescence at  $d_{bin} \sim r_b$  takes the longest time.

### $3.2.3. \ Implications$

As can be seen in our analytic derivation, the timescale for the inspiral of a binary planetesimal is dependent on its environment and on the binary properties. Figure 4 shows the binary merger timescale as a function of small planetesimal size for a range of big planetesimal sizes and separations from the star. To make this figure, we calculate the integral  $\langle F_D \rangle = \int_0^{2\pi} F_D(v_{rel}) d\theta$  numerically with  $v_{rel} = v_{bin} \sin \theta + v_{disk}$ , using the full expression for  $F_D$  embodied in Equation (7). This, for example, allows the relevant drag law to vary as a function of  $\theta$ if appropriate. We choose either the merger timescale evaluated at  $d_{bin} = min(R_H, R_{WS})$  or at  $d_{bin} = r_b$ , whichever is larger. We maintain our assumption of circular orbits. This assumption is only valid for merger timescales longer than of order the orbital period of the binary around the Sun,  $P_{\text{orb}}$ . The assumption that  $m_s v_{bin}/F_{D,disk} \gg P_{bin}$  breaks down for binaries with large bodies smaller than ~100m-1km in size, making our (already short) merger timescales upper limits in these cases.

We find that binary planetesimals over a wide range of masses inspiral and likely merge in times much shorter than the typical lifetimes of gaseous protoplanetary disks. Binary asteroids with components having radii less than a few tens of km have been observed in the main belt (e.g., Richardson & Walsh 2006). Such pairs were not likely to survive for long in a gaseous disk (see top and middle panels of Figure 4). Observed binary TNOs, however, have radii larger than a few tens of km (e.g., Noll et al. 2008), and could have survived for more than a Myr (bottom panel of Figure 4). If binary minor planets formed in the primordial gas disk (e.g. as suggested by Nesvorný et al. 2010), those with small components are less likely to have survived to this day. Given this formation scenario, the orbital characteristics of even the largest binary asteroids likely changed due to their evolution in gas. The currently observed orbital properties of binary asteroids (Naoz et al. 2010) are therefore unlikely to reflect only their properties at birth; e.g. binaries born with wide separations were likely to inspiral into more compact configurations. While the orbits of currently observed binary TNOs were likely unaffected, as binary TNOs with smaller components are found, this effect will need to be considered.

## 4. OTHER ASPECTS OF GAS-PLANETESIMAL INTERACTIONS

As we suggested above, the WISH radius can have important implications for gas-planetesimal interactions. In this study we mainly focused on the implications of the WISH radius for binary planetesimals. However, this scale could be important for other processes, similar to the role played by the Hill radius in gas-free environments. Here we only briefly mention these issues, which will be discussed in detail (and more quantitatively) elsewhere.

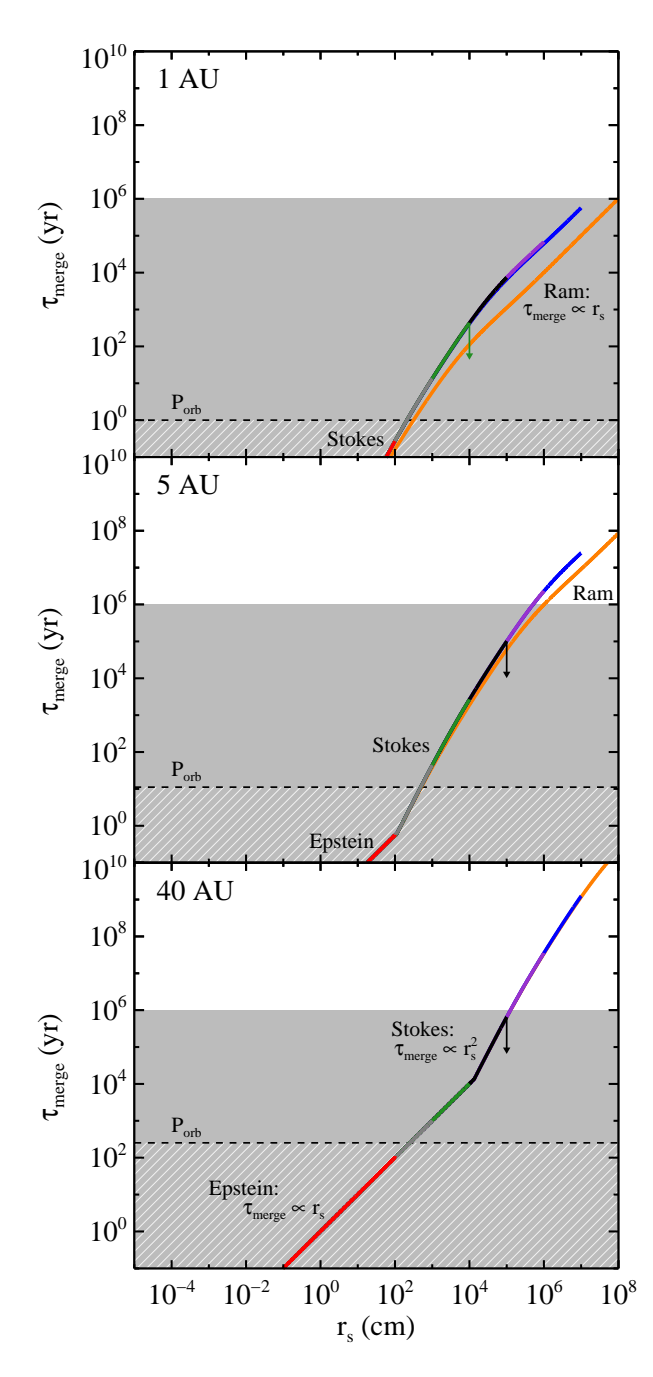


Figure 4. Merger timescales,  $\tau_{\rm merge}$  for binaries located 1 (top), 5 (middle), and 40 (bottom) AU from their host stars, as a function of the radius of the smaller binary component,  $r_s$ . Binary planetesimals with a wide range of masses inspiral and likely merge on timescales shorter than the typical lifetimes of protoplanetary disks (gray region). Colors correspond to different large planetesimal sizes, matching the colors in Figure 2. For large planetesimals with radii  $r_b \lesssim 10^3 {\rm km}$ , the merger time is independent of  $r_b$ . The merger time is reduced for  $r_b = 10^3 {\rm km}$  (orange, lower curve) as the ram pressure drag regime becomes important. For  $r_b < 100 {\rm m}$  (top) or 1km (middle and bottom), our assumption that  $m_s v_{bin}/F_{D,disk} \gg P_{\rm bin}$  breaks down, and our curves are upper limits. Timescales shorter than the orbital period around the star,  $P_{\rm orb}$ , (hashed region) indicate that inspiral will not occur on circular orbits and a more detailed calculation is required.

Gas-drag induced capture and coagulation of planetesimals: Two unbound planetesimals may dissipate some of their kinetic energy during an encounter (due to gas-drag), and may become bound to form a transitional binary. Such binaries could then continue to inspiral and finally merge due to gas drag (as discussed in the previous section). This capture-coalescence process, which could play a role in the build up and coagulation of planetesimals will be discussed in detail elsewhere (Murray-Clay and Perets, in preparation; see also the settling regime discussed by Ormel & Klahr, 2010).

Planetesimal erosion: As shown above, in some regimes the WISH radius is smaller than the big planetesimal size. This would suggest that under these conditions wind-shearing may blow away loose parts from the surface of single planetesimals, if they are weakly bound to the planetesimal (e.g. pieces from aggregates held together only by gravity could be blown from the surface of the main component of the planetesimals). Indeed, such erosion of planetesimals was experimentally observed for dust aggregates (Paraskov et al. 2006).

Post impact evolution of planetesimals: Following the collisions of two planetesimals some of their material may be ejected from the surface. A large fraction of this material is still gravitationally bound to the system. However, small size particles gravitationally bound to larger planetesimals could be blown away by the wind, if they are ejected beyond the WISH radius. The post-impact evolution of these particles could therefore be qualitatively different than the corresponding non-gaseous collisional evolution, prohibiting the smallest impact debris particles from ever accreting to the main bodies of the planetesimals. Nevertheless, wind may also induce re-accretion of ejecta material in some cases (Teiser & Wurm 2009), depending on the ejecta trajectory. In addition, the short merger timescales we find for binary planetesimals, suggest that any (WISHstable) bound debris around the main collision remnant would inspiral and accrete to the main body.

Planetesimal encounters and collisions in a gaseous environment: The collision rates between planetesimals vary for different regimes of velocity and encounter distances scales, where one of the most important scales of the problem is the Hill radius (e.g., Goldreich et al. 2004). The WISH radius provides an additional important parameter for planetesimal encounters, which has to be taken into account in order to determine the outcome of planetesimal encounters in gas. Recently (and independently) Ormel & Klahr (2010) discussed planetesimal encounters in a gaseous environment for some specific encounter regimes, and provided detailed calculations for these regimes. Our study suggests an additional and complementary understanding of these issues.

#### 5. SUMMARY

In this study we explored the differential gas-drag acceleration between different size planetesimals in a gaseous environment. We defined the wind-shearing radius as the distance at which the differential acceleration between two close-by planetesimals is comparable to their mutual gravitational pull. Planetesimal interactions close to or beyond this limit would be strongly affected by wind shearing. The wind-shearing radius has

important implications for the existence and survival of binaries. We find that binary planetesimals cannot form or survive with separations beyond this scale, even if this separation is smaller than the Hill radius, as they would be destabilized and sheared apart by the head wind. WISH-stable binary planetesimal are also affected by gas

drag, and can inspiral and coalesce in times shorter than the lifetime of the gaseous disk. The wind-shearing radius may have important implications for planetesimal evolution, in particular planetesimal erosion, post impact evolution of planetesimals, and planetesimal encounters and coagulation. These effects merit further investigation.

#### APPENDIX

## WIND-SHEARING DISRUPTION OF BINARY PLANETESIMALS : PARAMETER DEPENDENCE

In the following we provide a more detailed discussion on the dpendence of the WISH stability criterion for binary planetesimals on their environment and properties.

### Gas density and relative velocity

The gaseous environment and the velocities of planetesimals with respect to the gas likely change with time in a given disk, and vary across planetary systems. Therefore, the WISH radius and the stability of binary planetesimals and satellites is time and system dependent. These issues are illustrated in Figure 5, which shows how the WISH radius varies as a function of the relative velocity and gas density. The figure shows the WISH stability radius of an  $r_b = 10$  km planetesimal at 1 AU, for various choices of the relative planetesimal-gas velocity (upper panel) and the gas density (lower panel). Note that for small planetesimals in the Stokes regime the WISH radius becomes independent of the gas-density, as can be seen in Eq. (12), and the various lines in Figure 5 converge. We do not show the dependence of  $R_{WS}$  on temperature since it is weak (at most  $R_{WS} \propto c_s^{-1/2} \propto T^{-1/4}$ ; see Eq. 12).

As might be expected, the general trend of the WISH radius is to be smaller for higher gas densities and/or higher planetesimal velocities relative to the gas, i.e. WISH becomes more pronounced with stronger gas drag. Also, as mentioned before, very large comparable size planetesimals are hardly affected by gas-drag and the WISH radius becomes larger than their Hill radius. Taken together, the WISH will be more important for smaller binary planetesimals, during earlier stages of their growth/evolution, in a more gas-rich environment; WISH gradually becomes negligible at later stages.

#### REFERENCES

Andrews, S. M., Wilner, D. J., Hughes, A. M., Qi, C., & Dullemond, C. P. 2010, ApJ, 723, 1241 Brown, P. P. & Lawler, D. F. 2003, Journal of Environmental Engineering, 129, 222 Cheng, N.-S. 2009, Powder Technology, 189, 395 Chiang, E. & Youdin, A. N. 2010, Annual Review of Earth and Planetary Sciences, 38, 493 Chiang, E. I. & Goldreich, P. 1997, ApJ, 490, 368 Goldreich, P., Lithwick, Y., & Sari, R. 2004, ARAA, 42, 549 Hamilton, D. P. & Burns, J. A. 1991, Icarus, 92, 118 Lissauer, J. J. 1993, ARAA, 31, 129 Murray-Clay, R. A. & Schlichting, H. E. 2011, Accepted to ApJ Nakagawa, Y., Sekiya, M., & Hayashi, C. 1986, Icarus, 67, 375 Naoz, S., Perets, H. B., & Ragozzine, D. 2010, ApJ, 719, 1775 Nelson, R. P. & Gressel, O. 2010, MNRAS, 409, 639 Nesvorný, D., Youdin, A. N., & Richardson, D. C. 2010, AJ, 140, 785 Noll, K. S. et al. 2008, in The Solar System Beyond Neptune, 345–363 Ormel, C. W. & Klahr, H. H. 2010, A&A, 520, A43+ Paraskov, G. B., Wurm, G., & Krauss, O. 2006, ApJ, 648, 1219 Parker, A. H. & Kavelaars, J. J. 2010, ApJ, 722, L204 Perets, H. B. 2010, ApJL, in press (arXiv:1012.0567) Perets, H. B. & Naoz, S. 2009, ApJl, 699, L17 Richardson, D. C. & Walsh, K. J. 2006, Annual Review of Earth and Planetary Sciences, 34, 47 Shen, Y. & Tremaine, S. 2008, AJ, 136, 2453 Teiser, J. & Wurm, G. 2009, A&A, 505, 351 Weidenschilling, S. J. 1977, MNRAS, 180, 57 Whipple, F. L. 1973, NASA Special Publication, 319, 355

Youdin, A. N. 2010, in EAS Publications Series, Vol. 41, EAS Publications Series, ed. T. Montmerle, D. Ehrenreich, & A.-M. Lagrange, 187–207

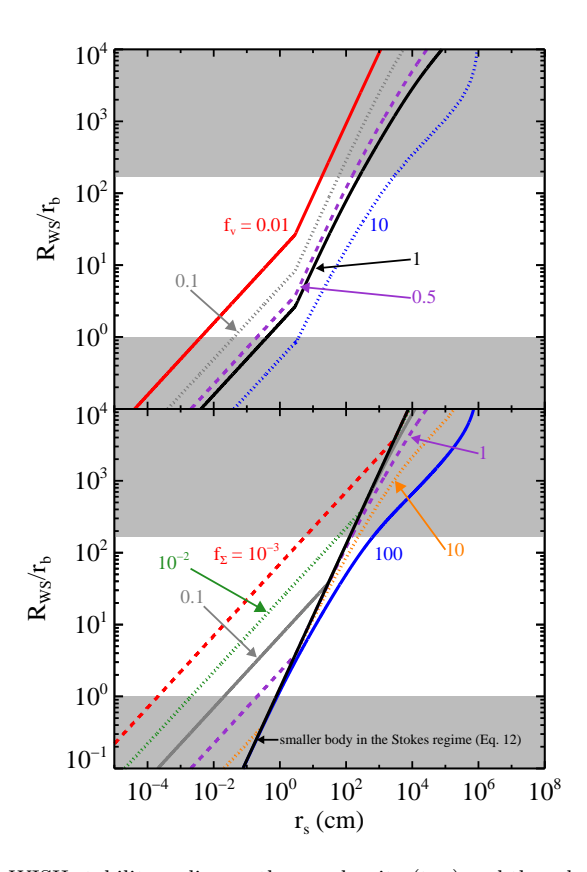


Figure 5. Dependence of the the binary WISH stability radius on the gas-density (top) and the relative velocity between the planetesimals and the gas (bottom). These figures show the dependence for a specific choice of the big planetesimal,  $r_b = 10$  km at 1 AU in our fiducial disk. The density and velocity for each line in the upper and lower panels, respectively, are  $\Sigma = f_{\Sigma} \times 2 \times 10^3$  g cm<sup>-2</sup> and  $v_{rel} = f_v \times 0.5 c_s^2/v_K$ . The dashed lines in both panels correspond to the same parameters used for the respective lines for the 10 km size big planetesimals shown in Figs. 1 and 2. Shaded regions correspond to separations beyond the Hill radius (upper region) or below the physical radius of the big planetesimals (lower region).